



Close-in Exoplanets as Candidates for Strange Quark Matter Objects

Abudushataer Kuerban^{1,2} , Jin-Jun Geng^{1,2} , Yong-Feng Huang^{1,2} , Hong-Shi Zong^{3,4,5}, and Hang Gong⁶

¹ School of Astronomy and Space Science, Nanjing University, Nanjing 210023, People's Republic of China; hyf@nju.edu.cn, gengjinjun@nju.edu.cn, lompa46@163.com

² Key Laboratory of Modern Astronomy and Astrophysics (Nanjing University), Ministry of Education, Nanjing 210023, People's Republic of China

³ Department of Physics, Nanjing University, Nanjing 210093, People's Republic of China

⁴ Department of Physics, Anhui Normal University, Wuhu, Anhui 241000, People's Republic of China

⁵ Nanjing Proton Source Research and Design Center, Nanjing 210093, People's Republic of China

⁶ National Astronomical Observatories, Chinese Academy of Sciences, Beijing 100101, People's Republic of China

Received 2019 August 19; revised 2019 December 22; accepted 2020 January 7; published 2020 February 11

Abstract

Since the true ground state of hadrons may be strange quark matter (SQM), pulsars may actually be strange stars rather than neutron stars. According to this SQM hypothesis, strange planets can also stably exist. The density of normal matter planets can hardly be higher than 30 g cm^{-3} . They will be tidally disrupted when the orbital radius is less than $\sim 5.6 \times 10^{10} \text{ cm}$, or when the orbital period (P_{orb}) is less than $\sim 6100 \text{ s}$. However, an SQM planet can safely survive even when it is very close to the host, due to its high density. This feature can help us identify SQM objects. Here, we have tried to search for SQM objects among close-in exoplanets orbiting around pulsars. It is found that four pulsar planets (XTE J1807-294 b, XTE J1751-305 b, PSR 0636 b, PSR J1807-2459A b) completely meet the criterion of $P_{\text{orb}} < 6100 \text{ s}$, and are thus good candidates for SQM planets. The periods of two other planets (PSR J1719-14 b and PSR J2051-0827 b) are only slightly larger than the criterion value. They could be regarded as potential candidates. Additionally, we find that the periods of five white dwarf planets (GP Com b, V396 Hya b, J1433 b, WD 0137-349 b, and SDSS J1411+2009 b) are less than 0.1 day; they might also be SQM planets. Gravitational wave emissions from these close-in planetary systems are calculated from the view of various gravitational wave detectors.

Unified Astronomy Thesaurus concepts: Gravitational waves (678); Pulsars (1306); Neutron stars (1108); Exoplanet systems (484)

1. Introduction

Soon after the discovery of neutrons, the existence of neutron stars (NSs), which are mainly made up of neutrons, was predicted. In the 1960s, pulsars were discovered. As extremely compact objects with a typical mass of $\sim 1.4M_{\odot}$ and a typical radius of only about 10 km, they were soon identified as neutron stars. However, it has also been argued that the ground state of matter at extreme densities may actually be quark matter (Itoh 1970; Bodmer 1971) rather than the hadronic form. The internal composition of these extremely compact stars thus is still largely unclear. For instance, under such an extreme condition, some particles like hyperons, baryons, and even bosons may appear; quark deconfinement may also occur. In particular, it has long been suggested that even more exotic states such as strange quark matter (SQM) may exist in the core (Itoh 1970; Bodmer 1971; Farhi & Jaffe 1984; Witten 1984). Recently, the discovery of several $2M_{\odot}$ pulsars (Demorest et al. 2010; Antoniadis et al. 2013; Cromartie et al. 2020) has attracted attention. Pulsars with such a high mass and a small radius imply that the density at the center can reach several times nuclear saturation density, which further complicates the internal composition of these compact stars.

Following the SQM hypothesis, the existence of a whole sequence of SQM objects, such as strange quark stars (SSs) (Farhi & Jaffe 1984; Witten 1984; Alcock et al. 1986), strange quark dwarfs (Glendenning et al. 1995a, 1995b), and strange quark planets (Glendenning et al. 1995a, 1995b; Xu & Wu 2003; Horvath 2012; Huang & Yu 2017) have been predicted. For example, Jiang et al. (2018) argued that the

double white dwarf (WD) binary J125733.63+542850.5 may actually contain two strange dwarfs. SQM objects may be covered by a thin crust of normal hadronic matter, or may even simply be bare SQM cores (Glendenning et al. 1995a, 1995b). The common compact nature of SSs and NSs makes it difficult to discriminate these two kinds of internally different stars observationally (Alcock et al. 1986). A few efforts have been made to reveal the difference between them. For example, they may have different M – R relations (Witten 1984; Krivoruchenko & Martem'ianov 1991; Glendenning et al. 1995a; Li et al. 1995; de Avellar & Horvath 2010; Drago et al. 2014), and SSs may rotate much faster (with spin period $P_{\text{spin}} < 1 \text{ ms}$) than NSs (Friedman et al. 1989; Frieman & Olinto 1989; Glendenning 1989; Kristian et al. 1989; Sawyer 1989; Madsen 1998; Dai & Lu 1995a, 1995b; Bhattacharyya et al. 2016). They may also have different cooling rates (Pizzochero 1991; Page & Applegate 1992; Ma et al. 2002), different gravitational wave (GW) features (Jaranowski et al. 1998; Madsen 1998; Lindblom & Mendell 2000; Andersson et al. 2002; Jones & Andersson 2002; Bauswein et al. 2010; Moraes & Miranda 2014; Geng et al. 2015; Mannarelli et al. 2015), and different maximum masses (Lai & Xu 2009; Li et al. 2010; Weissenborn et al. 2011; Mallick 2013; Zhu et al. 2013; Zhou et al. 2018; Shibata et al. 2019). Nevertheless, due to the current impracticability of the above methods, the problem remains unsolved.

Encouragingly, several new methods were recently proposed to distinguish SSs from NSs. The basic idea involves the tremendous difference between SQM planets and normal matter ones. Because of its extreme compactness, an SQM planet can be very close to its host SS star without being tidally

disrupted. It can even emit strong GW signals when it finally spirals-in and merges with the host star (Geng et al. 2015). GW emission from these merging SQM planets within our Galaxy can be detected by GW detectors such as advanced LIGO and the future Einstein Telescope. It is thus suggested that we could identify SQM objects by searching for very close-in planets around pulsars (Huang & Yu 2017), or by detecting GW bursts from merging SQM planet systems (Geng et al. 2015).

It is interesting to note that nearly 10 GW events from merging double black holes (and even one from merging double neutron stars) have been detected by advance LIGO and Virgo since 2016 (Abbott et al. 2016, 2017). Recently, advanced LIGO has just begun a new observational run, which will surely come up with many more GW events. It is hoped that the great breakthrough in GW astronomy will shed light on possible detection of GW emission from merging SQM planet systems in the near future. At the same time, rapid progress in observational technology has led to a drastic increase in the number of extrasolar planets being detected in recent decades. Interestingly, a good number of exoplanets are found to be orbiting around pulsars. In this study, we examine these pulsar planets systematically to search for very close-in ones that could be ideal candidates for SQM objects. The possibility of detecting GW emission from these candidates will also be explored.

The structure of our paper is as follows. In Section 2, the background relevant to SQM planet systems is briefly introduced. In Section 3, we describe the data source of our sample. In Section 4, SQM candidates are selected and evaluated by considering the criteria for close-in introduced in Section 2. GW emission from the candidate SQM planet systems is calculated and compared with the limiting sensitivities of current and future GW experiments in Section 5. In Section 6, we discuss the cases where the SQM planets are covered by a normal matter crust. Finally, Section 7 presents our conclusions and a discussion.

2. Theories Relevant to SQM Planet Systems

SSs can be composed of bare SQM, but they can also have a normal matter crust. For an SQM star with a mass of $\sim 1\text{--}1.6 M_\odot$, the thickness of the crust is usually several hundred meters and the crust mass would be as small as $\sim 10^{-5} M_\odot$ (Alcock et al. 1986; Glendenning et al. 1995a, 1995b; Huang & Lu 1997). But for an SQM planet, the crust would be much thicker and its mass could even be larger than the SQM core. In this study, we first assume that the SQM planet is a bare strange quark object for simplicity. Then in Section 6, we also briefly discuss the cases where SQM planets are embedded in a normal matter crust.

2.1. Criteria for Identifying SQM Planets

The tidal disruption radius of a planet by its host star mainly depends on the mean density ($\bar{\rho}$) of the planet and the mass of the central host star (M). It can be expressed as $r_{\text{td}} \approx (6M/\pi\bar{\rho})^{1/3}$ (Hills 1975), and can be rewritten as

$$r_{\text{td}} \approx 2.37 \times 10^6 \left(\frac{M}{1.4M_\odot} \right)^{1/3} \times \left(\frac{\bar{\rho}}{4 \times 10^{14} \text{ g cm}^{-3}} \right)^{-1/3} \text{ cm.} \quad (1)$$

Assuming that the host star is a typical pulsar with a mass of $1.4M_\odot$, if the planet is an SQM planet with an extremely high mean density of $4 \times 10^{14} \text{ g cm}^{-3}$, then it will be disrupted only when its orbital radius is less than $2.37 \times 10^6 \text{ cm}$, i.e., when it almost comes to the surface of the host pulsar.

In contrast, exoplanets composed of normal matter typically have a density of $\leq 1\text{--}10 \text{ g cm}^{-3}$ so that they would be tidally disrupted if they are too close to their host (Huang & Yu 2017). Taking 30 g cm^{-3} as a safe upper limit for normal planets, then the limiting disruption radius can be calculated as $5.6 \times 10^{10} \text{ cm}$ from Equation (1) (Huang & Yu 2017). In this study, we take this value as a criterion to distinguish normal planets and SQM ones. If a planet is observed to have an orbital radius (a) smaller than $5.6 \times 10^{10} \text{ cm}$, then it is most likely an exotic strange quark object, but not a normal matter planet. According to Kepler's law, such a close-in planet should also have a very small orbital period, $P_{\text{orb}} \lesssim 6100 \text{ s}$ (Huang & Yu 2017). Therefore, we could identify candidates for SQM planets using the criteria of $P_{\text{orb}} \lesssim 6100 \text{ s}$ and/or $a \lesssim 5.6 \times 10^{10} \text{ cm}$.

2.2. GWs from SQM Planet Systems

According to general relativity, the orbital motion of a binary system can lead to GW emission and spiral-in of the system. The GW emission power of a system with known masses and orbital parameters is

$$L_{\text{GW}} = \frac{32G^4}{5c^5} \frac{M^2 m^2 (M + m)}{a^5} F(e), \quad (2)$$

where c is the speed of light, G is the gravitational constant, and m is the mass of the planet. The factor $F(e) = \left(1 + \frac{73}{24}e^2 + \frac{37}{96}e^4\right)/(1 - e^2)^{7/2}$ is a function of the orbital eccentricity (e). Here we take $F(e) = 1$ for circular orbits considered in our modeling.

In a binary system, the orbit will evolve with time due to continuous GW emission. During this process, the GW strain will increase with time. If the distance of the binary system with respect to us is d , then the strain amplitude of the GW can be expressed as (Peters & Mathews 1963; Postnov & Yungelson 2014; Geng et al. 2015)

$$h = 5.1 \times 10^{-23} \left(\frac{M_C}{1 M_\odot} \right)^{5/3} \left(\frac{P_{\text{orb}}}{1 \text{ hr}} \right)^{-2/3} \left(\frac{d}{10 \text{ kpc}} \right)^{-1}, \quad (3)$$

where $M_C = (Mm)^{3/5}/(M + m)^{1/5}$ is the chirp mass. A directly observable quantity of GW is the strain spectral amplitude. For a binary system, it is given as (Finn & Chernoff 1993; Nissanke et al. 2010; Postnov & Yungelson 2014; Geng et al. 2015)

$$h_f = 6.4 \times 10^{-21} \left(\frac{M_C}{1 M_\odot} \right)^{5/6} \left(\frac{f}{300 \text{ Hz}} \right)^{-7/6} \times \left(\frac{d}{10 \text{ kpc}} \right)^{-1} \text{ Hz}^{-1/2}, \quad (4)$$

where $f = 2/P_{\text{orb}}$ is the GW frequency, which evolves with time. Note that the GW frequency f is twice the orbital motion frequency.

Because of the continuous energy loss through GW emission, the system will coalesce at the final stage of the inspiraling process. The coalescence timescale (Peters &

Table 1
Candidate Pulsar Planets and Their Host Pulsars

Planet Name	Mass m (M_{jup})	P_{orb} (day)	Host Name	Distance d (pc)	Mass M (M_{\odot})	References
Gold sample						
PSR 0636 b	8	0.067	PSR J0636	210	1.4	1, 2, 3
PSR J1807-2459A b	9.4	0.07	PSR J1807-2459A	2790	1.4	4, 5, 6, 7
PSR 1719-14 b	1	0.090706293	PSR 1719-14	1200	1.4	3, 8, 9
PSR J2322-2650 b	0.7949	0.322963997	PSR J2322-2650	230	1.4	3
PSR 1257+12 b	0.00007	25.262	PSR 1257+12	710	1.4	10, 11, 12, 13, 14
PSR 1257+12 c	0.013	66.5419	PSR 1257+12	710	1.4	10, 11, 12, 13, 14
PSR 1257+12 d	0.012	98.2114	PSR 1257+12	710	1.4	10, 11, 12, 13, 14
PSR B0943+10 b	2.8	730	PSR B0943+10	890	1.5	15
PSR B0943+10 c	2.6	1460	PSR B0943+10	890	1.5	15
PSR B0329+54 b	0.0062	10139.34	PSR B0329+54	1000	1.4	16, 17, 18
PSR B1620-26(AB) b	2.5	36525	PSR B1620-26(AB)	3800	1.35	19, 20, 21, 22, 23
Silver sample						
PSR J2051-0827 b	28.3	0.099110266	PSR J2051-0827	1280	1.4	7, 24
PSR J2241-5236 b	12	0.14567224	PSR J2241-5236	500	1.35	7, 25
PSR B1957+20 b	22	0.38	PSR B1957+20	1530	1.4	7, 26
Copper sample						
XTE J1807-294 b	14.5	0.0278292	XTE J1807-294	5500	1.5	27, 28, 29, 30, 31, 32
XTE J1751-305 b	27	0.02945997	XTE J1751-305	11000	1.7	33, 34, 35
PSR J1544+4937 b	18	0.12077299	PSR J1544+4937	3500	1.7	36, 37
PSR J1446-4701 b	23	0.277666077	PSR J1446-4701	1500	1.4	38, 39, 40
PSR J1502-6752 b	26	2.48445723	PSR J1502-6752	4200	1.4	38, 39

References. (1) Stovall et al. (2014), (2) Spiewak et al. (2016), (3) Spiewak et al. (2018), (4) D’Amico et al. (2001), (5) Ransom et al. (2001), (6) Lynch et al. (2012), (7) Ray & Loeb (2017), (8) Bailes et al. (2011), (9) Martin et al. (2016), (10) Wolszczan & Frail (1992), (11) Wolszczan (1994), (12) Wolszczan (2012), (13) Patruno & Kama (2017), (14) Wolszczan (2018), (15) Suleymanova & Rodin (2014), (16) Demianski & Proszynski (1979), (17) Shabanova (1995), (18) Starovoit & Rodin (2017), (19) Thorsett et al. (1993), (20) Lewis et al. (2008), (21) Mottez & Heyvaerts (2011), (22) Schneider et al. (2011), (23) Veras (2016), (24) Stappers et al. (1996), (25) Keith et al. (2011), (26) Reynolds et al. (2007), (27) Markwardt et al. (2003a, 2003b), (28) Campana et al. (2003), (29) Kirsch et al. (2004), (30) Falanga et al. (2005), (31) Riggio et al. (2007), (32) Patruno et al. (2010), (33) Markwardt et al. (2002), (34) Gierliński & Poutanen (2005), (35) Andersson et al. (2014), (36) Bhattacharyya et al. (2013), (37) Tang et al. (2014), (38) Keith et al. (2012), (39) Ng et al. (2014), (40) Arumugasamy et al. (2015).

Mathews 1963; Peters 1964; Lorimer 2008) of the system is expressed as

$$t_{\text{co}} = 9.88 \times 10^6 \text{yr} \left(\frac{P_{\text{orb}}}{1 \text{ hr}} \right)^{8/3} \left(\frac{\mu}{1 M_{\odot}} \right)^{-1} \left(\frac{\mathcal{M}}{1 M_{\odot}} \right)^{-2/3}, \quad (5)$$

where $\mu = Mm/(M + m)$ is the reduced mass and $\mathcal{M} = M + m$ is the total mass of the system.

3. Data Collection

In this study, we will systematically examine all the available short-period exoplanets to search for possible candidate SQM planets. For this purpose, we have searched through various exoplanet databases. Currently, popular exoplanet databases that are widely used in the field include: the Extrasolar Planets Encyclopaedia (hereafter EU⁷), the NASA Exoplanet Archive (ARCHIVE⁸), the Open Exoplanet Catalogue (OPEN⁹), the Exoplanet Data Explorer (ORG¹⁰), and the Extrasolar Planets catalog produced by Kyoto University (EXOKyoto¹¹). The numbers of planets in these databases are very different from

each other. Interestingly, note that a detailed comparison of these databases has been carried out by Bashi et al. (2018). Generally speaking, EU seems to provide the most complete sample for exoplanets. There are 6699 planets listed on the EU website, among which 4011 are confirmed and 2688 are candidates.

Since SQM planets are most likely to be found orbiting around pulsars (in this case, the pulsars themselves should also be strange stars, but not normal neutron stars), we will mainly concentrate on pulsar planets. So, as the initial step, we first select all the candidates of pulsar planets. In this aspect, the EU database contributes most of the objects. There are 18 pulsar planets listed in EU, six listed in ARCHIVE, and three listed in ORG. The total number of pulsar planet candidates is 19 after considering the overlap in different databases. In Table 1, we have listed some key parameters of these 19 candidates as well as their host pulsars. Among these objects, six planets interestingly have an orbital period less than 0.1 day (i.e., 8640 s). Note that our exact period criterion for SQM objects is 6100 s, but we believe that all the planets with $P_{\text{orb}} < 0.1$ days deserve to be paid special attention.

The nature of companions around pulsars is actually not easy to define clearly. A companion of several Jupiter masses could be a massive planet, but it could also be a small WD. The key problem is that its radius usually cannot be accurately measured. As a result, we should bear in mind that the 19

⁷ <http://www.exoplanet.eu/>

⁸ <https://exoplanetarchive.ipac.caltech.edu/>

⁹ <http://www.openexoplanetcatalogue.com/>

¹⁰ <http://www.exoplanets.org/>

¹¹ <http://www.exoplanetkyoto.org/catalog/?lang=en>

Table 2
White Dwarf Planets with $P_{\text{orb}} < 0.1$ Day and Their Host Stars

Planet Name	Mass m (M_{jup})	P_{orb} (day)	Host Name	Distance d (pc)	Mass M (M_{\odot})	References
GP Com b	26.2	0.032	GP Com	75	0.33	1, 2, 3, 4
V396 Hya b	18.3	0.045	V396 Hya	77	0.32	2, 3, 4, 5
J1433 b	57.1	0.054	J1433	226	0.8	3, 4, 6, 7
WD 0137-349 b	56	0.07943002	WD 0137-349	102.26	0.39	8, 9, 10, 11
SDSS J1411+2009 b	50	0.0854	SDSS J1411+2009	177	0.53	12, 13, 14

References. (1) Nather et al. (1981), (2) Kupfer et al. (2016), (3) Wong et al. (2019), (4) Cunha et al. (2018), (5) Ruiz et al. (2001), (6) Littlefair et al. (2006), (7) Santisteban et al. (2016), (8) Maxted et al. (2006), (9) Burleigh et al. (2006), (10) Casewell et al. (2015), (11) Longstaff et al. (2017), (12) Drake et al. (2010), (13) Beuermann et al. (2013), (14) Littlefair et al. (2014).

objects listed in Table 1 are only candidates, not confirmed pulsar planets. According to the confidence level, we have divided these 19 objects into three classes, the gold sample, the silver sample, and the copper sample. In the gold sample, there are strong clues supporting the objects as planets. In the silver sample, there are some clues hinting at the objects as planets (Ray & Loeb 2017). In the copper sample, the objects might be planets, but the evidence supporting the idea is highly lacking. Interestingly, we find that three objects in the gold sample and one object in the silver sample have periods less than 0.1 day. We will describe the details of these objects in the next section.

SQM planets may also exist around WDs, because these so-called WDs might actually be strange quark dwarfs. So, we also select all the WD planets that have an orbital period less than 0.1 day from EU. The total number of WD planets meeting this requirement is five, as listed in Table 2.

To get an overall picture on how these short-period planets differ from others, we plot all the planets with available masses and orbital periods on the m - P_{orb} plane in Figure 1. It clearly shows that all the planets with a period smaller than 0.1 day are orbiting around pulsars or WDs. These kinds of ultra-short-period objects form a distinct group and take a special place in the lower right region of Figure 1. This strongly hints that they may have an exotic nature as compared with other planets.

4. Candidates for SQM Planets

As explained in Section 2.1, because of its extreme compactness, an SQM object could be very close to its host strange star, without being tidally disrupted. So, closeness is a unique feature of SQM planets. To search for SQM objects, we have selected all the close-in exoplanets around pulsars and WDs. These ultra-short-period (less than 0.1 day) objects are listed in Table 3. To resist tidal disruption, they should have a relatively high mean density. To see how exotic these objects are, we have calculated their minimum mean densities using the period-density relation $\rho_{\text{min}} \approx 3\pi/(0.462^3 GP_{\text{orb}}^2)$ (Frank et al. 1985; Bailes et al. 2011). The results are also presented in Table 3. We can see that the minimum densities of these objects are all significantly larger than that of normal rocky or iron material (typically $1\text{--}10\text{ g cm}^{-3}$). If these objects are planets and not small WDs, then the possibility that they are SQM objects is very high. Below, we will examine these close-in objects one by one in detail and try to clarify their true nature.

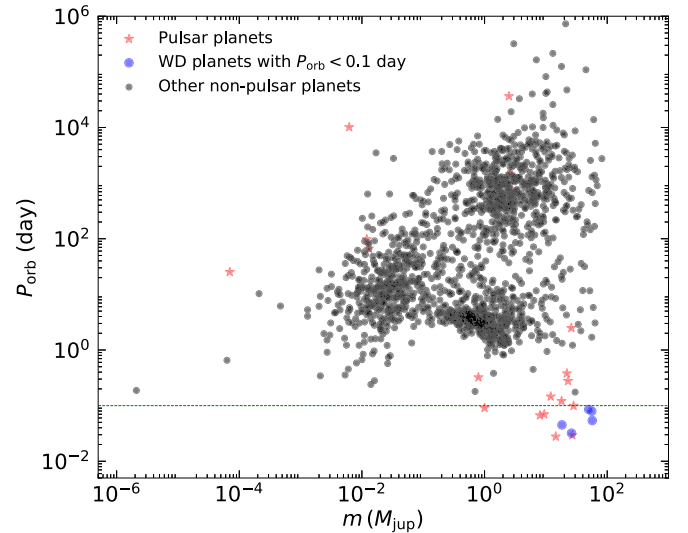


Figure 1. Orbital periods vs. masses for all the 1638 exoplanets with data available from the EU website (<http://www.exoplanet.eu/catalog/>). The red stars represent candidate pulsar planets. The blue points correspond to the five close-in white dwarf planets with $P_{\text{orb}} < 0.1$ days, and the black dots represent the other 1616 exoplanets.

Table 3
Orbital Parameters and Minimum Mean Densities of Ultra-short-period Objects

Planet Name	P_{orb} (s)	Orb. Radius a (10^{10} cm)	ρ_{min} (g cm^{-3})
XTE J1807-294 b	2404	3.1	247.9
XTE J1751-305 b	2545	3.4	221.2
PSR 0636 b	5789	5.4	42.8
PSR J1807-2459A b	6048	5.6	39.2
PSR 1719-14 b	7837	6.6	23.3
PSR J2051-0827 b	8563	7.1	19.5
GP Com b	2765	2.1	187.5
V396 Hya b	3888	2.6	94.8
J1433 b	4666	4.0	65.8
WD 0137-349 b	6863	4.1	30.4
SDSS J1411+2009 b	7379	4.7	26.3

4.1. Close-in Objects around Pulsars

The mass of planets can be distributed over a very wide range. Some planets can be very massive. In fact, the upper mass limit has been derived by many authors, and could be $43_{-23}^{+14} M_{\text{jup}}$ (Grether & Lineweaver 2006), $24 M_{\text{jup}}$ (Wright et al. 2011), $25 M_{\text{jup}}$ (Schneider et al. 2011), $42.5 M_{\text{jup}}$ (Ma & Ge 2014), or $60 M_{\text{jup}}$ (Hatzes & Rauer 2015). On the other

hand, WDs cannot be too small and they should have a lower mass limit. Recently, two low-mass WDs were reported, i.e., SDSS J184037.78+642312.3 ($0.17M_{\odot}$) (Hermes et al. 2012) and SDSS J222859.93+362359.6 ($0.16M_{\odot}$) (Hermes et al. 2013). They hint that WDs may be unlikely to be less than $100 M_{\text{jup}}$. In our Table 1, all the objects are significantly less massive than the planetary mass limits, thus are reasonable candidates for planets.

Among all the close-in candidates in Table 3, three are gold sample objects, one is a silver sample object, and two are copper sample objects. The other five are WD planet candidates. Here, we describe these objects one by one.

4.1.1. Gold Sample Objects

PSR J0636 b is a companion of the millisecond pulsar PSR J0636+5129 (spin period 2.87 ms) (Stovall et al. 2014). It has a mass of $8M_{\text{jup}}$. Its orbital period is ~ 5789 s, and the orbital radius is correspondingly $\sim 5.4 \times 10^{10}$ cm. PSR J0636+5129 does not exhibit any eclipses caused by excess material in the system (Stovall et al. 2014; Spiewak et al. 2016; Kaplan et al. 2018). PSR J0636 b is clearly identified as a planet by many authors (Stovall et al. 2014; Spiewak et al. 2016, 2018). It is also explicitly listed as a planet by several planet databases, such as by EU, EXOKyoto, PHLUPR (Planetary Habitability Laboratory of the University of Puerto Rico at Arecibo¹²), and GCEXO (General Catalogue of EXOplanets¹³).

PSR J1807-2459A b is a companion of the millisecond pulsar PSR J1807-2459A (spin period 3.06 ms) (D’Amico et al. 2001; Ransom et al. 2001; Lynch et al. 2012). This object has a mass of $9.4M_{\text{jup}}$, with an orbital period of ~ 6048 s, and correspondingly an orbital radius of $\sim 5.6 \times 10^{10}$ cm. PSR J1807-2459A shows no eclipses, but one cannot rule out the possibility of eclipses at longer wavelengths (Ransom et al. 2001; Lynch et al. 2012). PSR J1807-2459A b is identified as a planet by several authors (D’Amico et al. 2001; Ray & Loeb 2017). Websites including this object in their planet catalogs are EU, EXOKyoto, PHLUPR, and GCEXO.

PSR 1719-14 b is a companion of the millisecond pulsar PSR J1719-1438 (spin period 5.7 ms) (Bailes et al. 2011; Martin et al. 2016). It has a mass of $1M_{\text{jup}}$, with an orbital period of ~ 7837 s, and an orbital radius of $\sim 6.6 \times 10^{10}$ cm. It is identified as a planet by many researchers (Bailes et al. 2011; Martin et al. 2016; Spiewak et al. 2018). Websites listing this object in their planet catalogs are EU, ARCHIVE, EXOKyoto, PHLUPR, and GCEXO. PSR J1719-14 b was once considered to be a C/O dwarf in an ultra-compact low-mass X-ray binary by Bailes et al. (2011). However, since its mass is very low ($1M_{\text{jup}}$), it is more likely to be a planetary object. Horvath (2012) explicitly argued that PSR J1719-14 b should be an exotic strange object rather than a C/O dwarf. Very recently, Huang & Yu (2017) also identified PSR J1719-14 b as an ideal candidate for a SQM planet.

4.1.2. Silver Sample Objects

PSR J2051-0827 b is a companion of the millisecond pulsar PSR J2051-0827 (spin period 4.5 ms) (Stappers et al. 1996; Ray & Loeb 2017). It has a mass of $28.3M_{\text{jup}}$, with an orbital period of ~ 8563 s, and an orbital radius of $\sim 7.1 \times 10^{10}$ cm. Its

mass is within the planetary mass range. While Ray & Loeb (2017) suggested this object as a planet, it has also been argued that it might be a brown dwarf (Stappers et al. 1996). Websites including this object as a planet in catalogs are EU, ARCHIVE, EXOKyoto, PHLUPR, and GCEXO. The orbital period and orbital radius of this object are slightly larger than our strange planet criteria, but we suggest that it might be a good candidate for an SQM object and deserves special attention.

4.1.3. Copper Sample Objects

XTE J1807-294 b is a companion of the millisecond X-ray pulsar XTE J1807-294 (spin period 5.25 ms) (Campana et al. 2003; Markwardt et al. 2003a, 2003b; Kirsch et al. 2004; Falanga et al. 2005; Riggio et al. 2007; Patruno et al. 2010). It has a mass of $14.5 \pm 8.5M_{\text{jup}}$, with an orbital period of ~ 2404 s, and an orbital radius of $\sim 3.1 \times 10^{10}$ cm. No X-ray eclipse was observed from this system (Falanga et al. 2005). According to the mass–radius relation, the companion may be the core of a previously crystallized C/O dwarf (Deloye & Bildsten 2003). However, there are no emission or absorption lines found from this companion (Campana et al. 2003). This object is listed as a planet in EU and EXOKyoto, but its true nature is still highly unclear.

XTE J1751-305 b is a companion of the millisecond X-ray pulsar XTE J1751-305 (spin period 2.3 ms) (Markwardt et al. 2002; Gierliński & Poutanen 2005; Andersson et al. 2014). It has a mass of $27 \pm 10M_{\text{jup}}$, with an orbital period of ~ 2545 s, and an orbital radius of $\sim 3.4 \times 10^{10}$ cm. The pulsar shows no X-ray eclipses during observations (Markwardt et al. 2002; Gierliński & Poutanen 2005). This object is listed as a planet in EU and EXOKyoto, but several authors have also argued that it may be the core of a previously crystallized C/O dwarf (Deloye & Bildsten 2003).

The orbital parameters of both XTE J1807-294 b and XTE J1751-305 b well satisfy our SQM criteria. Also, it is obvious that the masses of both objects are within the planet mass range. Although their true nature is still uncertain, we note that Horvath (2012) have argued that an exotic strange object interpretation is the best alternative to a C/O dwarf interpretation for these two objects. We believe that the likelihood of these two objects being SQM planets is high. They need to be studied in more detail in the future.

4.2. Close-in Objects Around WDs

GP Com b is a companion of the WD GP Com (Nather et al. 1981; Kupfer et al. 2016). Its mass is $26.2 \pm 16.6M_{\text{jup}}$, with an orbital period of ~ 2765 s, and an orbital radius of $\sim 2.1 \times 10^{10}$ cm (Kupfer et al. 2016). There are suggestions that it may be a degenerated He dwarf (Nather et al. 1981). But the observed abundances of Ne line from this object could be affected by crystallization processes in the core, and this excludes a highly evolved He donor nature for it (Kupfer et al. 2016). Alternatively, it was argued to be a planet by many authors (Cunha et al. 2018; Wong et al. 2019). Websites listing this object as a planet are EU, EXOKyoto, PHLUPR, and GCEXO.

V396 Hya b is a companion of the WD V396 Hya (Ruiz et al. 2001; Kupfer et al. 2016). Its orbital period is ~ 3888 s, and its orbital radius is $\sim 2.6 \times 10^{10}$ cm. Its mass is measured as $18.3 \pm 12.2M_{\text{jup}}$ (Kupfer et al. 2016). It was suggested to be a degenerated He dwarf (Ruiz et al. 2001), or a crystallized Ne

¹² <http://phl.upr.edu/projects/habitable-exoplanets-catalog/top10>

¹³ <http://www.exoplanet.info/index.html>

core (Kupfer et al. 2016). However, other authors (Cunha et al. 2018; Wong et al. 2019) have argued that it could be a planet. Websites listing this object as a planet are EU, EXOKyoto, and PHLUPR.

J1433 b is a companion of the WD SDSS J143317.78 +101123.3 (WD J1433) (Littlefair et al. 2006; Santisteban et al. 2016). It has an orbital period of ~ 4666 s, and an orbital radius of $\sim 4.0 \times 10^{10}$ cm. Its mass is $57 \pm 0.7 M_{\text{jup}}$. It was argued to be a planet by several research groups (Cunha et al. 2018; Wong et al. 2019). Websites listing this object as a planet are EU, EXOKyoto, and PHLUPR. However, note that a few other authors suggested that this object may be an irradiated brown dwarf (Santisteban et al. 2016).

WD 0137-349 b is a companion of the WD 0137-349 (Burleigh et al. 2006; Maxted et al. 2006; Littlefair et al. 2014; Casewell et al. 2015; Longstaff et al. 2017). It has a mass of $56 \pm 6 M_{\text{jup}}$, with an orbital period of ~ 6863 s, and an orbital radius of $\sim 4.1 \times 10^{10}$ cm. This object is listed as a planet in the EU and EXOKyoto databases. But again note that it was suggested to be an irradiated brown dwarf by several authors (Burleigh et al. 2006; Maxted et al. 2006).

SDSS J1411+2009 b is a companion of the WD SDSS J141126.20+200911.1 (WD J1411). It has a mass of $50 \pm 2.0 M_{\text{jup}}$, with an orbital period of ~ 7379 s and an orbital radius of $\sim 4.7 \times 10^{10}$ cm (Drake et al. 2010; Beuermann et al. 2013; Littlefair et al. 2014). It is listed as a planet in the EU and EXOKyoto databases, but several authors have also suggested it is an irradiated brown dwarf (Beuermann et al. 2013).

Orbital parameters of the above five close-in objects around WDs satisfy the criterion of $P_{\text{orb}} < 0.1$ day. Their masses are also within the planetary mass range. However, the planetary nature of these objects is still debatable. In particular, they may actually be brown dwarfs. Here, we give some more discussion on this point. In fact, there is no clear boundary between the masses of planets and brown dwarfs. It is well known that the mass of brown dwarfs can range from the deuterium-burning limit ($0.013 M_{\odot}$ ($\sim 13 M_{\text{jup}}$)) to the hydrogen-burning limit ($0.072 M_{\odot}$ ($\sim 75 M_{\text{jup}}$)). The property of a close-in companion is usually seriously affected by the irradiation from its host since it is generally tidally locked (Demory & Seager 2011; Laughlin et al. 2011; Burgasser et al. 2019). This effect is quite similar for both brown dwarfs and giant planets, thus could not be easily used to distinguish them (Faherty et al. 2013). However, we notice that three of the five objects have extremely small orbital periods. They are GP Com b, V396 Hya b, and J1433 b, and their orbital periods are 2765 s, 3888 s, and 4666 s, respectively. As a result, their minimal possible mean densities are 187.5 g cm^{-3} , 94.8 g cm^{-3} , and 65.8 g cm^{-3} , respectively. Their density is so high that they can hardly be normal brown dwarfs. We argue that at least these three objects are very good candidates for SQM planets.

5. GWs from SQM Planetary Systems

According to general relativity, a binary system continuously emits GW signals due to the orbital motion of the companion. This will lead to an evolution of the orbit, and cause the GW emission power to increase gradually. At some stage of this gradual process, GW detectors such as LISA (Laser Interferometer Space Antenna) will be able to detect the GW signals from these systems (Cunha et al. 2018; Wong et al. 2019).

For close-in companions orbiting around their hosts, GW emission may be a powerful tool to probe their nature. In this

Table 4
GW Luminosity, Strain Amplitude, and Coalescence Time Scale for the Planetary Systems in Our Sample

Planet Name	L_{GW} (egr s^{-1})	h	t_{co} (yr)
XTE J1807-294 b	3.8×10^{30}	2.2×10^{-24}	1.9×10^8
XTE J1751-305 b	1.3×10^{31}	2.1×10^{-24}	1.1×10^8
PSR 0636 b	5.7×10^{28}	1.7×10^{-23}	3.7×10^9
PSR J1807-2459A b	6.7×10^{28}	1.5×10^{-24}	3.5×10^9
PSR 1719-14 b	3.2×10^{26}	3.0×10^{-25}	6.6×10^{10}
PSR J2051-0827 b	1.9×10^{29}	7.5×10^{-24}	3.0×10^9
PSR J1544+4937 b	5.2×10^{28}	1.7×10^{-24}	6.9×10^9
PSR J2241-5236 b	9.1×10^{27}	6.2×10^{-24}	2.0×10^{10}
PSR J1446-4701 b	4.1×10^{27}	2.6×10^{-24}	5.7×10^{10}
PSR J2322-2650 b	3.0×10^{24}	5.4×10^{-25}	2.4×10^{12}
PSR B1957+20 b	1.3×10^{27}	2.0×10^{-24}	1.4×10^{11}
PSR J1502-6752 b	3.5×10^{24}	2.5×10^{-25}	1.7×10^{13}
PSR 1257 12 b	1.1×10^{10}	8.4×10^{-31}	3.1×10^{21}
PSR 1257 12 c	1.5×10^{13}	8.2×10^{-29}	2.2×10^{20}
PSR 1257 12 d	3.6×10^{12}	5.8×10^{-29}	6.7×10^{20}
PSR B0943+10 b	2.7×10^{14}	3.0×10^{-27}	5.8×10^{20}
PSR B0943+10 c	2.3×10^{13}	1.7×10^{-27}	4.0×10^{21}
PSR B0329+54 b	1.8×10^5	9.7×10^{-31}	3.1×10^{26}
PSR B1620-26(AB) b	4.0×10^8	4.3×10^{-29}	2.4×10^{25}
GP Com b	9.9×10^{29}	9.5×10^{-23}	4.2×10^8
V396 Hya b	1.5×10^{29}	5.1×10^{-23}	1.5×10^9
J1433 b	2.7×10^{30}	8.7×10^{-23}	4.3×10^8
WD 0137-349 b	2.6×10^{29}	8.9×10^{-23}	2.0×10^9
SDSS J1411+2009 b	2.6×10^{29}	5.4×10^{-23}	2.2×10^9

section, we first calculate the persistent GW emissions from the candidate SQM systems in our sample and evaluate the possibility of their being detected by the LISA observatory. Then, we also calculate the strength of the catastrophic GW bursts when the candidate SQM systems finally merge due to continuous GW emissions, and compare the results with those from relevant GW detectors.

5.1. Persistent GWs from SQM Planet Systems

For all the planetary systems in our sample, we have calculated their persistent GW luminosity and GW strain amplitude. The results are presented in Table 4. In Figure 2, we plot the GW luminosity versus the orbital radius for them. The red stars and blue points represent pulsar planets and WD planets, respectively. Generally speaking, the orbital radius is a key parameter determining the GW power. For those systems with the orbital radius being less than the critical tidal disruption radius of 5.6×10^{10} cm, the GW power is much stronger. Thus there is a hope that GW emission from these systems could be detected by our GW detectors.

In Figure 3, we plot the GW strain amplitude against GW frequency for the planetary systems in our sample. In this plot, the red stars represent pulsar planets and the blue points represent WD planets. The black line is the one-year integration sensitivity curve of LISA.¹⁴ Figure 3 shows clearly that three ultra-short-period systems (GP Com b, V396 Hya b and J1433 b) are lying above the sensitivity curve of LISA, thus may be detected by this powerful GW observatory. The two very close-in systems containing XTE J1807-294 b and XTE J1751-305 b are below the sensitivity curve, since their distances are still too large. If these two systems were located within a distance of

¹⁴ <http://www.srl.caltech.edu/~shane/sensitivity/index.html>

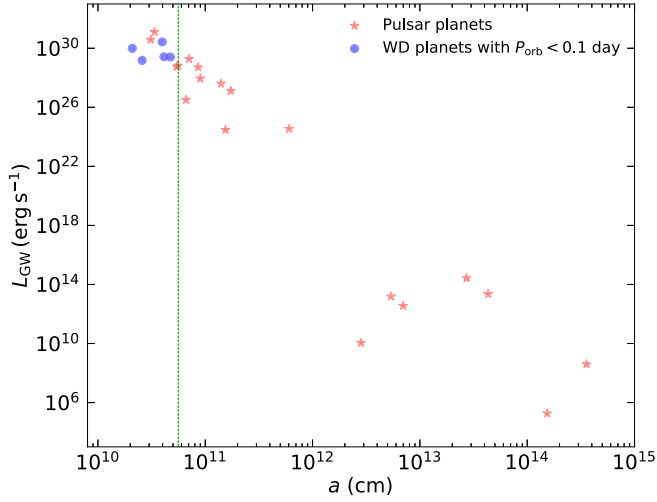


Figure 2. Power of gravitational wave emission vs. orbital radius for the planetary systems in our sample. The red stars are pulsar planets and the blue points are white dwarf planets with $P_{\text{orb}} < 0.1$ day. The vertical green dashed line marks the critical tidal disruption radius of $a = 5.6 \times 10^{10}$ cm for normal matter planets.

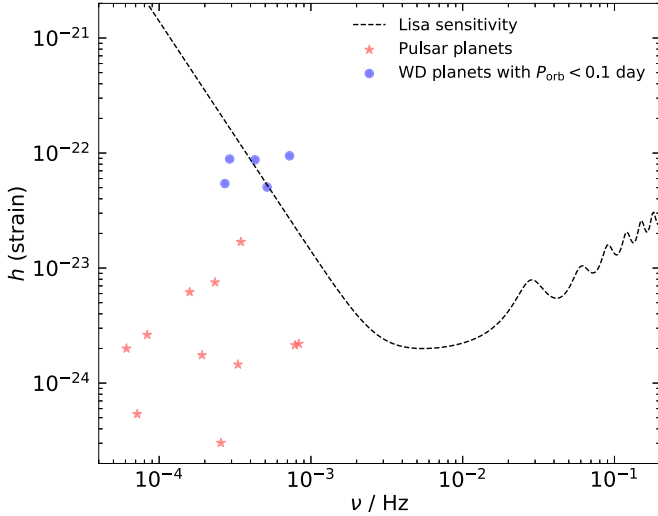


Figure 3. Gravitational wave strain amplitude vs. frequency for the planetary systems of our sample. The blue points represent white dwarf planets with $P_{\text{orb}} < 0.1$ day and the red stars represent pulsar planets. The black dashed line represents the sensitivity curve of LISA with a one-year integration time. For a similar plot, see Cunha et al. (2018) and Wong et al. (2019).

400 pc, then they would be detectable to LISA. For close-in planetary systems, GW observation can provide key information on the planet mass, orbital period, and orbital radius. We argue that GW observation would be a unique tool to search for SQM candidates. In the future, if a very close-in planet-like object (with mass being in the planet range, and orbital period significantly less than 6100 s) could be found orbiting around a stellar object through GW observations, then it must be an SQM planetary system.

5.2. GW Bursts from Merging SQM Planet Systems

Due to the self-gravity and strong self-bound force of SQM, an SQM planet can get very close to its host without being tidally disrupted by tidal forces. During the spiral-in process, the separation between the two objects decreases with time until they merge with each other. At the final merging stage, the

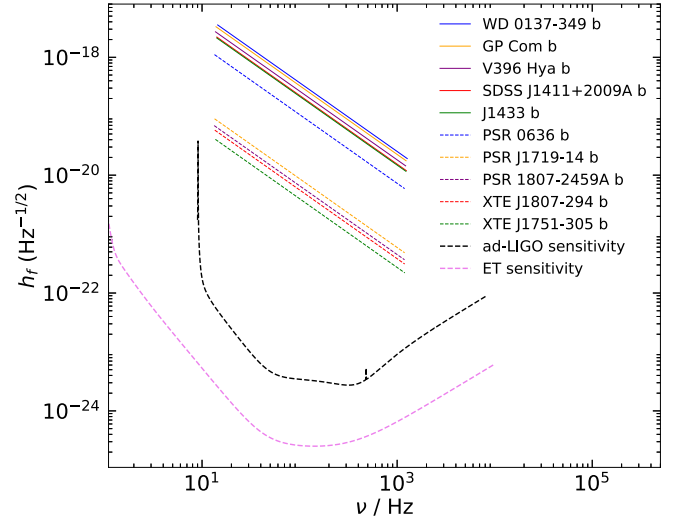


Figure 4. Strain spectral amplitude of the gravitational wave bursts for coalescing strange quark matter planet systems. The sensitivity curves of the advanced LIGO and Einstein Telescope are also plotted.

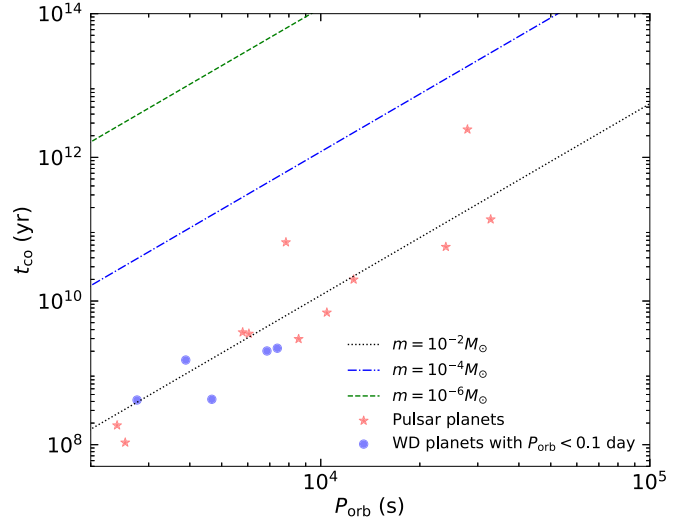


Figure 5. Coalescence timescale vs. the initial orbital period for the candidate strange quark matter planetary systems in our sample. Red stars correspond to pulsar planets and blue points correspond to white dwarf planets. The three straight lines illustrate the coalescence timescale for three different planet masses, with the host mass being set as $1.4M_{\odot}$.

system will give rise to a strong GW burst (Geng et al. 2015). In Figure 4, we plot the strain spectral amplitudes of the GW bursts that will be produced by several candidate SQM planetary systems. Note that these systems are at different distances, and the planets have different masses. For each system, we have used the actually observed parameters in the calculation. We see that the GW amplitudes are all well above the sensitivity curves of both the advanced LIGO and the Einstein Telescope, thus can potentially be detected by these instruments.

The energy loss rate due to GW emission is generally small as compared with the total kinetic energy of the planet. It may take a long time for a planetary system to finally merge. The merger timescale is mainly determined by the orbital radius and the planet mass. In Table 4, we have also calculated the coalescence timescales of the planetary systems in our sample. The results are illustrated in Figure 5. While most systems

essentially will not be able to merge even in the lifetime of the universe, there are about 10 close-in systems that would interestingly merge on a timescale of 10^8 – 10^9 yr. For example, the merger timescale is $\sim 10^8$ yr for the planetary systems of XTE J1807-294, XTE J1751-305, GP Com b, and J1433 b. Additionally, other factors may be involved and may lead to a much rapid merging process. For example, a pulsar may have multiple planets and the complicated interaction between these companions may speed up the merging processes of some objects (Huang & Geng 2014).

In short, merging of an SQM planet with its host pulsar can essentially happen on a predictable timescale in our Galaxy. GW emission from these events can be well detected by our current and future detectors. We suggest that searching for GW signals from merging planetary systems could be set as an important goal for the advanced LIGO and Einstein telescopes. This deserves extensive effort since it can provide a unique test for the SQM hypothesis.

6. SQM Planets with a Crust

It has been argued that SQM objects can also be embedded in a normal matter crust. The mass of these “dressed” SQM objects ranges from planetary mass to nearly two solar masses, forming the so-called strange-star/strange-dwarf sequence (Glendenning et al. 1995a, 1995b). In this section, we discuss the cases where the SQM planets have a normal matter crust.

The internal structure of a “dressed” SQM object is determined by two key parameters, the central density and the density at the bottom of the crust. The central density at the exact center of the whole star can be as high as a few times the nuclear saturation density of $\sim 4.0 \times 10^{14} \text{ g cm}^{-3}$. It determines the mass (M_{core}) and radius of the SQM core. For the normal matter at the bottom of the crust, it is usually believed that the maximum density cannot exceed the neutron drip density of $\rho_{\text{drip}} \approx 4.3 \times 10^{11} \text{ g cm}^{-3}$. At a density higher than this value, abundant free neutrons will appear and they will penetrate the outwardly directed electric field, falling onto the SQM core and being converted into SQM. As a result, a heavier crust cannot be supported by the electric field surrounding the SQM core. Note that a further study by Huang & Lu (1997) indicates that the maximum density at the crust bottom actually should be significantly smaller, i.e., no larger than $\rho_{\text{drip}}/5 \approx 8.3 \times 10^{10} \text{ g cm}^{-3}$. Their conclusion is drawn by considering the equilibrium between the supporting force from the electric field and the gravity of the whole crust.

In our study, we have solved the Tolman–Oppenheimer–Volkoff equation (Oppenheimer & Volkoff 1939) using the Runge–Kutta method to derive the properties of SQM objects with a normal matter crust. For normal matter in the crust (with density less than ρ_{drip}), we use the equation of state suggested by Baym et al. (1971). Our calculations are carried out assuming different initial values for the crust bottom density (ρ_{cb}) to investigate the effect of crusts of various thickness ($\rho_{\text{cb}} = 4.3 \times 10^{11} \text{ g cm}^{-3}$, $8.3 \times 10^{10} \text{ g cm}^{-3}$, 10^8 g cm^{-3} , 10^7 g cm^{-3} , 10^6 g cm^{-3} , 10^5 g cm^{-3} , and 10^4 g cm^{-3}). For each ρ_{cb} value, the SQM core mass (M_{core}) varies from $1.5M_{\odot}$ to $10^{-12}M_{\odot}$ to get a full strange-star/strange-dwarf sequence.

Figure 6 shows the relationship between the total mass (M_{tot}) and the radius (R_{tot}) of the sequence. In our plot, the vertical bar “|” marked with a letter “b” represents the lightest object in the sequence, and the cross symbol “x” marked with “c” indicates the largest-mass strange dwarf. The cross symbol “x” marked

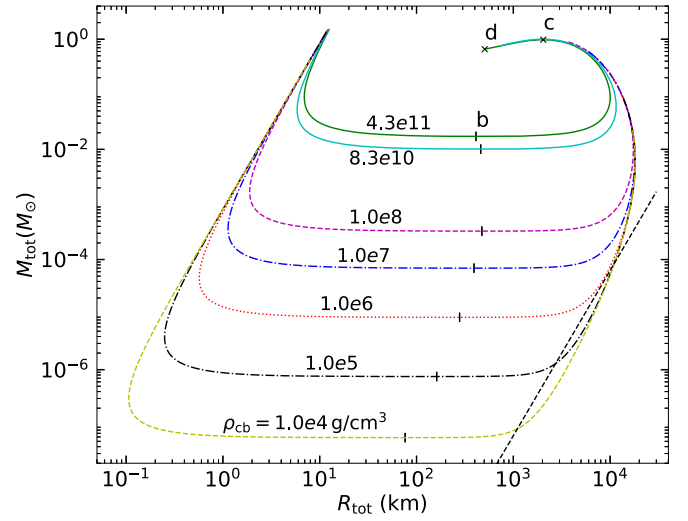


Figure 6. Mass–radius relation for the strange-star/strange-dwarf sequence. On each curve, the mass of the strange quark matter core shrinks from about $1.5 M_{\odot}$ to nearly zero from the left segment to the right segment. From top to bottom, the curves correspond to various crust bottom densities, with the density value (in units of g cm^{-3}) marked near the curve. For more details of the symbols, see the text.

with “d” is the endpoint of the sequence, as the SQM core shrinks to almost zero. According to the stability analysis of Glendenning et al. (1995a, 1995b), all the strange matter objects with $\rho_{\text{cb}} \leq 10^9 \text{ g cm}^{-3}$ are absolutely stable against radial oscillation. Additionally, for the SQM objects with $\rho_{\text{cb}} > 10^9 \text{ g cm}^{-3}$, only the segment between “c” and “d” is unstable (Glendenning et al. 1995a, 1995b). SQM planets usually have a mass significantly less than $0.1M_{\odot}$ and they surely will not appear in the “cd” segment, so they can all stably exist regardless of the bottom density. Note that in this figure, the straight dashed line at the lower right corner corresponds to the $M_{\text{tot}} \propto R_{\text{tot}}^3$ law with a constant density of 30 g cm^{-3} .

From Figure 6 we can see that when the crust bottom density is very high (for example, for the two lines with $\rho_{\text{cb}} = 4.3 \times 10^{11} \text{ g cm}^{-3}$ and $\rho_{\text{cb}} = 8.3 \times 10^{10} \text{ g cm}^{-3}$), even the lightest objects will have a mass larger than $0.01M_{\odot}$, which will be highly disputed as a planet mass. However, when the crust bottom density is low, such as for those lines with $\rho_{\text{cb}} \leq 10^8 \text{ g cm}^{-3}$, the lightest objects will be significantly less than $0.001M_{\odot}$. These low-mass objects are undoubtedly SQM planets. Note that in Figure 6, each strange-star/strange-dwarf sequence curve is characterized by a nearly horizontal segment. This means that, for an SQM planet with a given mass, it can either have a very small radius or a relatively large radius. For example, for a planetary SQM object of $0.001M_{\odot}$, the radius can be as small as 2–3 km. In this case, the object is mainly composed of dense quark matter, embedded in a very thin crust. On the other hand, it can also have a radius as large as 10^4 km. In this case, it will only have a very small SQM core, covered by a thick normal matter crust.

Since the tidal disruption radius of a planet is mainly determined by its density (see Equation (1)), we have calculated the mean density of the SQM stars in the strange-star/strange-dwarf sequence. Here the mean density is calculated by dividing the total mass of the star by its overall volume. Figure 7 illustrates the mean density versus radius. We see that as long as ρ_{cb} is larger than 10^6 g cm^{-3} , the mean

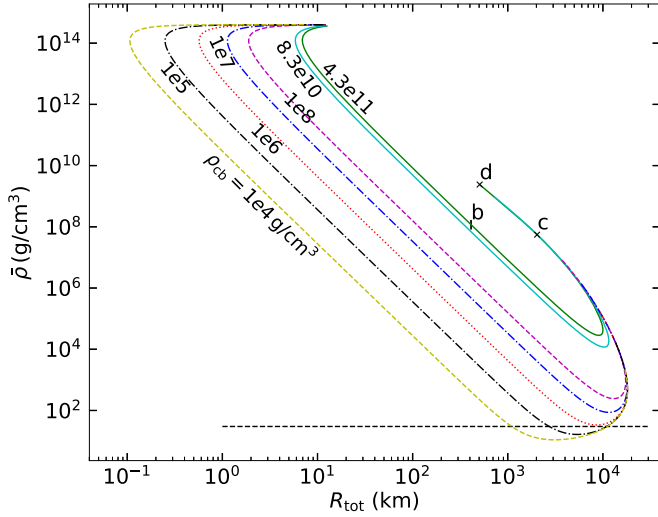


Figure 7. Mean density vs. radius for the strange-star/strange-dwarf sequence. Line styles and symbols are the same as those in Figure 6. The crust bottom density (in units of g cm^{-3}) is marked near each curve. The horizontal dashed line at the bottom corresponds to a mean density of 30 g cm^{-3} .

density will always be larger than 30 g cm^{-3} . Even in the cases of $\rho_{\text{cb}} \leq 10^5 \text{ g cm}^{-3}$, only a very small segment of the sequence will have a mean density less than 30 g cm^{-3} . Figure 8 plots the total mass versus mean density. It can be seen that the mean density of a crusted SQM planet can vary over a very wide range (between $\sim 10^2 \text{ g cm}^{-3}$ and $\sim 10^{14} \text{ g cm}^{-3}$), but is generally much larger than 30 g cm^{-3} . Figures 7 and 8 clearly show that SS planets with a normal matter crust are still very compact. They will safely survive even when the orbital radius is smaller than $\sim 5.6 \times 10^{10} \text{ cm}$ or when the orbital period is less than $\sim 6100 \text{ s}$. Note that in the rare cases where the SQM objects have a relatively small mean density (less than 30 g cm^{-3} , such as the lower right segment for $\rho_{\text{cb}} = 10^4 \text{ g cm}^{-3}$ and $\rho_{\text{cb}} = 10^5 \text{ g cm}^{-3}$ as in Figure 6), the planet can still survive as a close-in object to some extent after a complex form of tidal interaction. For these planets, only the not-so-dense crust will be markedly affected by the tidal force and might be essentially stripped off. The dense SQM core will be largely unaffected and will survive as a close-in bare SQM planet.

In Figure 9, we show the mass fraction ($M_{\text{core}}/M_{\text{tot}}$) of the SQM core versus the overall radius for the strange-star/strange-dwarf sequence. Generally speaking, if the crust has a negligible contribution to the star mass, then the object is predominantly made up of SQM ($M_{\text{core}}/M_{\text{tot}} \approx 1$) so that it will have a very small radius. On the other hand, if the SQM mass fraction is much less than 1, which means the object is mainly composed of normal hadronic matter, then the radius is usually as large as 10^3 – 10^4 km .

In short, from these plots, we see that SQM planets with a normal matter crust are generally very compact. They can still stably exist when they are quite close to their host. At the same time, the radii of these crusted SQM planets are significantly larger than those of bare SQM objects; this provides the interesting possibility of detecting them via more precise mass-radius measurements in the future. For example, they may be detectable via eclipsing effects due to their closeness, proximity, and relatively large radius. In this aspect, NASA's soft X-ray telescope on the *International Space Station*, Neutron Star Interior Composition Explorer, may be a powerful

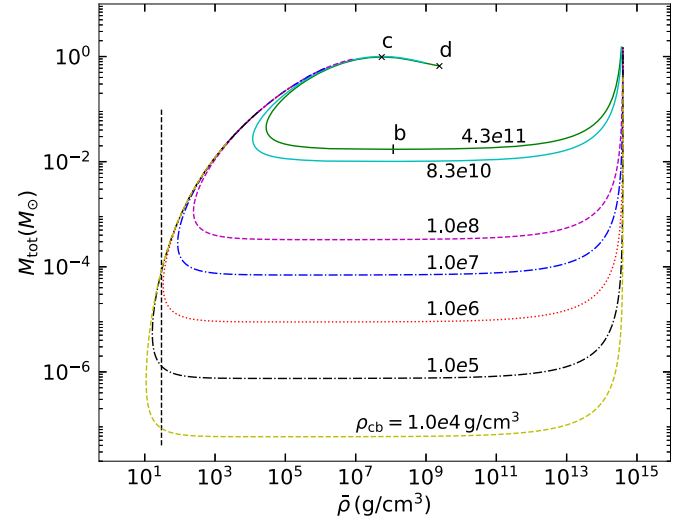


Figure 8. Total mass vs. mean density for the strange-star/strange-dwarf sequence. Line styles and symbols are the same as those in Figure 6. The crust bottom density (in units of g cm^{-3}) is marked near each curve. The vertical dashed line on the left corresponds to a mean density of 30 g cm^{-3} .

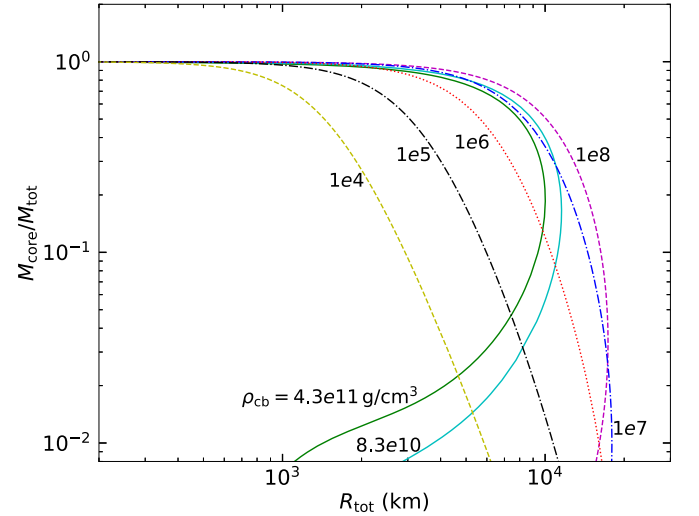


Figure 9. Mass fraction of the SQM core vs. radius for the strange-star/strange-dwarf sequence. Line styles and symbols are the same as those in Figure 6. The crust bottom density (in units of g cm^{-3}) is marked near each curve.

tool (Gendreau et al. 2016; Riley et al. 2019), and is expected to provide valuable clues. Some planned scientific missions like the future high-resolution space-based optical hypertelescopes have targeted neutron stars, pulsars, and exoplanets. The direct-imaging capability of hypertelescopes makes it possible to observe faint exoplanets near their bright parent star. Besides, extremely large telescopes (Snellen et al. 2015) can detect the optical emission of some pulsars (Shearer & Connor 2018; Malbet et al. 2019), so that we could search for optical transits caused by planets around pulsars, and could explore the physics of these systems. Some techniques such as the cross-correlation function method (Martins et al. 2015), the auto-correlation function method (Borra & Deschatelets 2018), and the independent component analysis method (Marcantonio et al. 2019) may be useful in measuring the mass and radius of planets.

7. Conclusions

In this study, we have tried to search for SQM planet candidates among extra-solar planetary systems. The criteria for SQM planets are set as $a < 5.6 \times 10^{10}$ cm and/or $P_{\text{orb}} < 6100$ s. A planet lying closer than this limit with respect to its host will need to have a density significantly larger than 30 g cm^{-3} to resist the tidal force, thus is unlikely a normal matter planet, but should be an SQM object. For SQM planets with a normal matter crust, our calculations indicate that generally they are compact enough that the above criteria still apply. As a result, we find that 11 objects are good candidates for SQM planets, including three gold sample objects, one silver sample object, two copper sample objects, and five WD companions. The three gold sample objects are PSR 0636 b, PSR J1807-2459A b, and PSR J1719-14 b. Their masses are all less than $10 M_{\text{Jup}}$ and their possibility of being a planetary object is very high. Among them, although PSR 1719-14 b has a period (7837 s) slightly larger than 6100 s, we still list it as a good candidate since it is essentially in a very close-in orbit. The silver sample object (PSR J2051-0827 b), the two copper sample objects (XTE J1807-294 b, XTE J1751-305b), and the five WD companions (GP Com b, V396 Hya b, J1433 b, WD 0137-349 b, SDSS J1411+2009 b) are all interesting candidates, but whether they are planetary objects or WDs is still somewhat uncertain and needs further clarification. We have also calculated the GW emissions from these systems. It is found that persistent GW emissions from at least three of them are detectable to LISA on a one-year integration. More encouragingly, GW bursts produced at the final merging stage by these candidate SQM planets are well above the sensitivity curves of the advanced LIGO and Einstein telescopes. GW observations thus could be a promising strategy for testing the SQM hypothesis.

It is striking to note that our SQM candidates are mainly found around millisecond pulsars. This leads to the interesting conjecture that there might be some intrinsic connection between SQM objects and low-mass X-ray binaries (LMXBs). Indeed, some authors (Li et al. 1995; Xu & Qiao 1998; Xu 2002; Poutanen & Gierliński 2003; Zhu et al. 2013) have tried to identify SSs in LMXBs. For example, the famous LMXBs of Her X-1 (Li et al. 1995) and SAX J1808.4-3658 have been argued as SS candidates (Li et al. 1999; Poutanen & Gierliński 2003; Gangopadhyay et al. 2012). Poutanen & Gierliński (2003) and Gangopadhyay et al. (2012) also noticed the similarity of XTE J1807-294 and XTE J1751-305 with respect to SAX J1808.4-3658 when they argued that SAX J1808.4-3658 should be a strange star. Furthermore, Gangopadhyay et al. (2013) listed 12 stars in binary systems as SSs, again including Her X-1 and SAX 1808.4-3658. Recently, Chen (2016) pointed out that the binary systems of SAX 1808.4-3658 and PSR J1719-1438 may have similar evolutionary history. In fact, the link between strange stars and LMXBs is not difficult to understand theoretically. Continuous accretion and significant mass transfer widely exists in LMXBs. Increasing the mass can easily lead to an ultra-high density at the center of the pulsar, leading to a phase transition and turning the pulsar into an SS even it is originally born as an NS.

Pulsars in the current close-in binary systems generally show no eclipsing in the high-frequency range. There are two possible reasons for this. First, the inclination angle of the orbit should be relatively large. Second, the density of the

companion may be high and its radius correspondingly very small. This will further support the SQM nature of the object. In several cases, the possible eclipse is reported to be observed at a low-frequency range. The small amount of eclipsing plasma in these cases may come from the ablation of the outer crust of the SQM planet.

How strange quark planets can be produced is an interesting issue. There are at least three possible channels. First, they may come from the SQM clumps formed in the early stage of the universe. According to the big bang theory, the universe goes through a quark era in its expansion history. At that time, both the temperature and the density are extremely high. Such a condition may directly give birth to some planetary mass SQM objects, which can survive up to now (Cottingham et al. 1994). The number of these objects may be enormous. After cooling down, they could even contribute a significant portion of dark matter as some kinds of dark compact objects in the universe (Chandra & Goyal 2000). They can also be captured by compact stars (and even by main-sequence stars), forming planetary systems. Second, the birth of an SQM host star itself may cause the formation of SQM planetary objects. SSs can be born during supernova explosions, or from merging of two compact stars, or from phase transition of massive NSs. All these processes are fierce explosive events and a large amount of SQM nuggets may be ejected from the new-born SS. The flux of SQM nuggets produced in this way in a typical galaxy is estimated as $\sim 0.1 \text{ cm}^{-2} \text{ s}^{-1}$ (Glendenning 1990; Glendenning & Weber 1992). These SQM nuggets can contaminate surrounding normal planets and convert them into SQM planets (Olinto 1987). It has been suggested that the two planets of PSR B1257+12 (Wolszczan & Frail 1992) may be formed in this way (Glendenning 1990; Caldwell & Friedman 1991; Glendenning et al. 1995b; Madsen 1999). Finally, a newborn SQM star is quite hot and highly turbulent. It may directly eject a large clump of SQM due to the joint effect of fast spinning and turbulence, forming an SQM planet outside (Xu & Wu 2003; Xu 2006; Horvath 2012). Note that SQM planets formed in this way are more likely close-in objects surrounding the compact host.

This work was supported by the National Natural Science Foundation of China (grant Nos. 11873030, 11475085, 11535005, 11690030, 11703041, and 11903019), by Nation Major State Basic Research and Development of China (2016YFE0129300), and by the Strategic Priority Research Program of the Chinese Academy of Sciences (“multi-waveband Gravitational Wave Universe,” grant No. XDB23040000).

ORCID iDs

Abudushataer Kuerban  <https://orcid.org/0000-0002-0786-7307>

Jin-Jun Geng  <https://orcid.org/0000-0001-9648-7295>

Yong-Feng Huang  <https://orcid.org/0000-0001-7199-2906>

Hang Gong  <https://orcid.org/0000-0001-8399-0780>

References

- Abbott, B. P., Abbott, R., Abbott, T. D., & Abernathy, M. R. 2016, *PhRvL*, **116**, 061102
- Abbott, B. P., Abbott, R., Abbott, T. D., Acernese, F., & Abernathy, M. R. 2017, *PhRvL*, **119**, 161101
- Alcock, C., Farhi, E., & Olinto, A. 1986, *ApJ*, **310**, 261

- Andersson, N., Jones, D. I., & Ho, W. C. G. 2014, *MNRAS*, **442**, 1786
- Andersson, N., Jones, D. I., & Kokkotas, K. D. 2002, *MNRAS*, **337**, 1224
- Antoniadis, J., Freire, P. C. C., Wex, N., et al. 2013, *Sci*, **340**, 448
- Arumugasamy, P., Pavlov, G. G., & Garmire, G. P. 2015, *ApJ*, **814**, 90
- Bailes, M., Bates, S. D., Bhalariao, V., et al. 2011, *Sci*, **333**, 1717
- Bashi, D., Helled, R., & Zucker, S. 2018, *Geosc*, **8**, 325
- Bauswein, A., Oechslin, R., & Janka, H.-T. 2010, *PhRvD*, **81**, 024012
- Baym, G., Pethick, C., & Sutherland, P. 1971, *ApJ*, **170**, 299
- Beuermann, K., Dreizler, S., Hessman, F. V., et al. 2013, *A&A*, **558**, A96
- Bhattacharyya, B., Roy, J., Ray, P. S., et al. 2013, *ApJL*, **733**, L12
- Bhattacharyya, S., Bombaci, I., Logoteta, D., & Thampan, A. V. 2016, *MNRAS*, **457**, 3101
- Bodmer, A. R. 1971, *PhRvD*, **4**, 1601
- Borra, E. F., & Deschatelets, D. 2018, *MNRAS*, **481**, 4841
- Burgasser, A., Baraffe, I., Browning, M., et al. 2019, arXiv:1903.04667
- Burleigh, M. R., Hogan, E., Dobbie, P. D., Napiwotzki, R., & Maxted, P. F. L. 2006, *MNRAS*, **373**, L55
- Caldwell, R., & Friedman, J. L. 1991, *PhLB*, **264**, 143
- Campana, S., Ravasio, M., Israel, G. L., Mangano, V., & Belloni, T. 2003, *ApJL*, **594**, L39
- Casewell, S. L., Lawrie, K. A., Maxted, P. F. L., et al. 2015, *MNRAS*, **447**, 3218
- Chandra, D., & Goyal, A. 2000, *PhRvD*, **62**, 063505
- Chen, W. C. 2016, *MNRAS*, **464**, 4673
- Cottingham, W. N., Kalafatis, D., & Mau, R. V. 1994, *PhRvL*, **73**, 1328
- Cromartie, H. T., Fonseca, E., Ransom, S. M., et al. 2020, *NatAs*, **4**, 72
- Cunha, J. V., Silva, F. E., & Lima, J. A. S. 2018, *MNRAS*, **480**, L28
- Dai, Z., & Lu, T. 1995a, *AcASn*, **36**, 165
- Dai, Z. G., & Lu, T. 1995b, *ChA&A*, **19**, 513
- D'Amico, N., Lyne, A. G., Manchester, R. N., Possenti, A., & Camilo, F. 2001, *ApJL*, **548**, L171
- de Avellar, M. G. B., & Horvath, J. E. 2010, *IJMPD*, **19**, 1937
- Deloye, C. J., & Bildsten, L. 2003, *ApJ*, **598**, 1217
- Demianski, M., & Proszynski, M. 1979, *Natur*, **282**, 383
- Demorest, P. B., Pennucci, T., Ransom, S. M., Roberts, M. S. E., & Hessels, J. W. T. 2010, *Natur*, **467**, 1081
- Demory, B. O., & Seager, S. 2011, *ApJS*, **197**, 12
- Drago, A., Lavagno, A., & Pagliara, G. 2014, *PhRvD*, **88**, 043014
- Drake, A. J., Beshore, E., Catelan, M., et al. 2010, arXiv:1009.3048
- Faherty, J. K., Rice, E. L., Cruz, K. L., Mamajek, E. E., & Núñez, A. 2013, *AJ*, **145**, 2
- Falanga, M., Bonnet-Bidaud, J. M., Poutanen, J., et al. 2005, *A&A*, **436**, 647
- Farhi, E., & Jaffe, R. L. 1984, *PhRvD*, **30**, 2379
- Finn, L. S., & Chernoff, D. F. 1993, *PhRvD*, **47**, 2198
- Frank, J., King, A. R., & Raine, D. J. 1985, *Accretion Power in Astrophysics* (Cambridge: Cambridge Univ. Press)
- Friedman, J. L., Ipser, J. R., & Parker, L. 1989, *PhRvD*, **62**, 3015
- Frieman, J. A., & Olinto, A. V. 1989, *Natur*, **341**, 633
- Gangopadhyay, T., Li, X. D., Ray, S., Dey, M., & Dey, J. 2012, *NewA*, **17**, 43
- Gangopadhyay, T., Ray, S., Li, X. D., & Dey, J. 2013, *MNRAS*, **431**, 3216
- Gendreau, K. C., Arzoumanian, Z., Adkins, P. W., et al. 2016, *Proc. SPIE*, **9905**, 99051H
- Geng, J. J., Huang, Y. F., & Lu, T. 2015, *ApJ*, **804**, 21
- Gierliński, M., & Poutanen, J. 2005, *MNRAS*, **359**, 1261
- Glendenning, N. K. 1989, *PhRvL*, **63**, 2629
- Glendenning, N. K. 1990, *MPLA*, **5**, 2197
- Glendenning, N. K., Kettner, C., & Weber, F. 1995a, *PhRvL*, **74**, 3519
- Glendenning, N. K., Kettner, C., & Weber, F. 1995b, *ApJ*, **450**, 253
- Glendenning, N. K., & Weber, F. 1992, *ApJ*, **400**, 647
- Grether, D., & Lineweaver, C. H. 2006, *ApJ*, **640**, 1051
- Hatzes, A. P., & Rauer, H. 2015, *ApJL*, **810**, L25
- Hermes, J. J., Montgomery, M. H., Gianninas, A., et al. 2013, *MNRAS*, **436**, 3573
- Hermes, J. J., Montgomery, M. H., Winget, D. E., et al. 2012, *ApJL*, **750**, L28
- Hills, J. G. 1975, *Natur*, **254**, 295
- Horvath, J. E. 2012, *RAA*, **12**, 813
- Huang, Y. F., & Geng, J. J. 2014, *ApJL*, **782**, L20
- Huang, Y. F., & Lu, T. 1997, *A&A*, **325**, 189
- Huang, Y. F., & Yu, Y. B. 2017, *ApJ*, **848**, 115
- Itoh, N. 1970, *PTPh*, **44**, 291
- Jaranowski, P., Królak, A., & Schutz, B. F. 1998, *PhRvD*, **58**, 063001
- Jiang, L., Chen, W. C., & Li, X. D. 2018, *MNRAS*, **476**, 109
- Jones, D. I., & Andersson, N. 2002, *MNRAS*, **331**, 201
- Kaplan, D. L., Stovall, K., Kerkwijk, M. H., Fremling, C., & Istrate, A. G. 2018, *ApJ*, **864**, 15
- Keith, M. J., Johnston, S., Bailes, M., et al. 2012, *MNRAS*, **419**, 1752
- Keith, M. J., Johnston, S., Ray, P. S., et al. 2011, *MNRAS*, **414**, 1292
- Kirsch, M. G. F., Mukerjee, K., Breitfellner, M. G., et al. 2004, *A&A*, **423**, L9
- Kristian, J., Pennypacker, C. R., Middledtrch, J., et al. 1989, *Natur*, **338**, 234
- Krivoruchenko, M. I., & Martem'ianov, B. V. 1991, *ApJ*, **378**, 628
- Kupfer, T., Steeghs, D., Groot, P. J., et al. 2016, *MNRAS*, **457**, 1828
- Lai, X. Y., & Xu, R. X. 2009, *MNRAS*, **398**, L31
- Laughlin, G., Crismani, M., & Adams, F. C. 2011, *ApJL*, **729**, L7
- Lewis, K. M., Sackett, P. D., & Mardling, R. A. 2008, *ApJL*, **685**, L153
- Li, A., Xu, R.-X., & Lu, J.-F. 2010, *MNRAS*, **402**, 2715
- Li, X. D., Bombaci, I., Dey, M., Dey, J., & van den Heuvel, E. P. J. 1999, *PhRvL*, **83**, 3776
- Li, X. D., Dai, Z. G., & Lu, T. 1995, *A&A*, **303**, L1
- Lindblom, L., & Mendell, G. 2000, *PhRvD*, **61**, 104003
- Littlefair, S. P., Casewell, S. L., Parsons, S. G., et al. 2014, *MNRAS*, **445**, 2106
- Littlefair, S. P., Dhillon, V. S., Marsh, T. R., et al. 2006, *Sci*, **314**, 1578
- Longstaff, E. S., Casewell, S. L., Wynn, G. A., Maxted, P. F. L., & Helling, C. 2017, *MNRAS*, **471**, 1728
- Lorimer, D. R. 2008, *LRR*, **11**, 8
- Lynch, R. S., Freire, P. C. C., Ransom, S. M., & Jacoby, B. A. 2012, *ApJ*, **745**, 109
- Ma, B., & Ge, J. 2014, *MNRAS*, **439**, 2781
- Ma, Z. X., Dai, Z. G., Huang, Y. F., & Lu, T. 2002, *Ap&SS*, **282**, 537
- Madsen, J. 1998, *PhRvL*, **81**, 3311
- Madsen, J. 1999, in *Hadrons in Dense Matter and Hadrosynthesis*, Vol. 516, ed. J. Cleymans, H. B. Geyer, & F. G. Scholtz (Berlin: Springer), 162
- Malbet, F., Abbas, U., Alves, J., et al. 2019, ESA Voyage 2050 white paper—Faint objects in motion: the new frontier of high precision astrometry, arXiv:1910.08028
- Mallick, R. 2013, *PhRvC*, **87**, 025804
- Mannarelli, M., Pagliaroli, G., Parisi, A., Pilo, L., & Tonelli, F. 2015, *ApJ*, **815**, 81
- Marcantonio, P. D., Morossi, C., Franchini, M., & Lehmann, H. 2019, *AJ*, **158**, 161
- Markwardt, C. B., Juda, M., & Swank, J. H. 2003a, *IAUC*, **8095**, 1
- Markwardt, C. B., Smith, E., & Swank, J. H. 2003b, *IAUC*, **8080**, 1
- Markwardt, C. B., Swank, J. H., Strohmayer, & Marshall, F. E. 2002, *ApJL*, **575**, L21
- Martin, R. G., Livio, M., & Palaniswamy, D. 2016, *ApJ*, **832**, 122
- Martins, J. H. C., Santos, N. C., Figueira, P., et al. 2015, *A&A*, **576**, A134
- Maxted, P. F. L., Napiwotzki, R., Dobbie, P. D., & Burleigh, M. R. 2006, *Natur*, **442**, 543
- Moraes, P. H. R. S., & Miranda, O. D. 2014, *MNRAS*, **445**, L11
- Mottez, F., & Heyvaerts, J. 2011, *A&A*, **532**, A21
- Nather, R. E., Robinson, E. L., & Stover, R. J. 1981, *ApJ*, **244**, 269
- Ng, C., Bailes, M., Bate, S. D., et al. 2014, *MNRAS*, **439**, 1865
- Nissanke, S., Holz, D. E., Hughes, S. A., Dalal, N., & Sievers, J. L. 2010, *ApJ*, **725**, 496
- Olinto, A. V. 1987, *PhLB*, **192**, 71
- Oppenheimer, J. R., & Volkoff, G. M. 1939, *PhRv*, **55**, 374
- Page, D., & Applegate, J. H. 1992, *ApJL*, **394**, L17
- Patruno, A., Hartman, J. M., Wijnands, R., Chakrabarty, D., & van der Klis, M. 2010, *ApJ*, **717**, 1253
- Patruno, A., & Kama, M. 2017, *A&A*, **608**, A147
- Peters, P. C. 1964, *PhRv*, **136**, B1224
- Peters, P. C., & Mathews, J. 1963, *PhRv*, **131**, 435
- Pizzochero, P. M. 1991, *PhRvL*, **66**, 2425
- Postnov, K. A., & Yungelson, L. R. 2014, *LRR*, **17**, 3
- Poutanen, J., & Gierliński, M. 2003, *MNRAS*, **343**, 1301
- Ransom, S. M., Greenhill, L. J., Herrnstein, J. R., et al. 2001, *ApJL*, **546**, L25
- Ray, A., & Loeb, A. 2017, *ApJ*, **836**, 135
- Reynolds, M. T., Callanan, P. J., Fruchter, A. S., et al. 2007, *MNRAS*, **379**, 1117
- Riggio, A., Salvo, T. D., Burderi, L., et al. 2007, *MNRAS*, **382**, 1751
- Riley, T. E., Watts, A. L., Bogdanov, S., et al. 2019, *ApJL*, **887**, L21
- Ruiz, M. T., Rojo, P. M., Garay, G., & Maza, J. 2001, *ApJ*, **552**, 679
- Santisteban, J. V. H., Knigge, C., Littlefair, S. P., et al. 2016, *Natur*, **533**, 366
- Sawyer, R. F. 1989, *PhLB*, **233**, 412
- Schneider, J., Dedieu, C., Sidaner, P. L., Savalle, R., & Zolotukhin, I. 2011, *A&A*, **532**, A79
- Shabanova, T. T. 1995, *ApJ*, **453**, 779
- Shearer, A., & Connor, E. O. 2018, in *IAU Symp. 337, Pulsar Astrophysics the Next Fifty Years*, ed. P. Weltevrede (Cambridge: Cambridge Univ. Press), 191
- Shibata, M., Zhou, E., Kiuchi, K., & Fujibayashi, S. 2019, *PhRvD*, **100**, 023015
- Snellen, I., de Kok, R., Birkby, J. L., et al. 2015, *A&A*, **576**, A59

- Spiewak, R., Bailes, M., Barr, E. D., et al. 2018, [MNRAS](#), **475**, 469
- Spiewak, R., Kaplan, D. L., Archibald, A., et al. 2016, [ApJ](#), **822**, 37
- Stappers, B. W., Bailes, M., Lyne, A. G., et al. 1996, [ApJL](#), **465**, L119
- Starovoi, E. D., & Rodin, A. E. 2017, [ARep](#), **61**, 948
- Stovall, K., Lynch, R. S., Ransom, S. M., et al. 2014, [ApJ](#), **791**, 67
- Suleymanova, S. A., & Rodin, A. E. 2014, [ARep](#), **58**, 796
- Tang, S., Kaplan, D. L., Phinney, E. S., et al. 2014, [ApJL](#), **791**, L5
- Thorsett, S. E., Arzoumanian, Z., & Taylor, J. H. 1993, [ApJL](#), **412**, L33
- Veras, D. 2016, [RSOS](#), **3**, 150571
- Virtanen, P., Gommers, R., Oliphant, T. E., et al. 2019, arXiv:1907.10121
- Weissenborn, S., Sagert, I., Pagliara, G., Hempe, M., & Bielich, J. S. 2011, [ApJL](#), **740**, L14
- Witten, E. 1984, [PhRvD](#), **30**, 272
- Wolszczan, A. 1994, [Ap&SS](#), **212**, 67
- Wolszczan, A. 2012, [NewAR](#), **56**, 2
- Wolszczan, A. 2018, in PSR B1257+12 and the First Confirmed Planets Beyond the Solar System, ed. H. J. Deeg & J. A. Belmonte (New York: Springer International Publishing AG), 21
- Wolszczan, A., & Frail, D. A. 1992, [Natur](#), **355**, 145
- Wong, K. W. K., Berti, E., Gabella, W. E., & Holley-Bockelmann, K. 2019, [MNRAS](#), **483**, L33
- Wright, J. T., Fakhouri, O., Marcy, G. W., et al. 2011, [PASP](#), **123**, 412
- Xu, R. X. 2002, [ApJL](#), **570**, L65
- Xu, R. X. 2006, [Aph](#), **25**, 212
- Xu, R. X., & Qiao, G. J. 1998, [ChPhL](#), **15**, 934
- Xu, R. X., & Wu, F. 2003, [ChPhL](#), **20**, 806
- Zhou, E. P., Zhou, X., & Li, A. 2018, [PhRvD](#), **97**, 083015
- Zhu, C. H., Lü, G. L., Wang, Z. J., & Liu, J. Z. 2013, [PASP](#), **125**, 25